

2016

# Near-threshold behavior of positronium-antiproton scattering

Ilya I. Fabrikant

*University of Nebraska-Lincoln*, ifabrikant@unl.edu

A. W. Bray

*Australian National University*

A. S. Kadyrov

*Curtin University*

I. Bray

*Curtin University*

Follow this and additional works at: <http://digitalcommons.unl.edu/physicsfabrikant>

---

Fabrikant, Ilya I.; Bray, A. W.; Kadyrov, A. S.; and Bray, I., "Near-threshold behavior of positronium-antiproton scattering" (2016). *Ilya Fabrikant Publications*. 10.

<http://digitalcommons.unl.edu/physicsfabrikant/10>

This Article is brought to you for free and open access by the Research Papers in Physics and Astronomy at DigitalCommons@University of Nebraska - Lincoln. It has been accepted for inclusion in Ilya Fabrikant Publications by an authorized administrator of DigitalCommons@University of Nebraska - Lincoln.

**Near-threshold behavior of positronium-antiproton scattering**

I. I. Fabrikant

*Department of Physics and Astronomy, University of Nebraska, Lincoln, Nebraska 68588-0299, USA*

A. W. Bray

*Theoretical Physics Department, Research School of Physics and Engineering, Australian National University, Canberra ACT 2601, Australia*

A. S. Kadyrov and I. Bray

*Curtin Institute for Computation and Department of Physics, Astronomy and Medical Radiation Science, Curtin University, GPO Box U1987, Perth, WA 6845, Australia*

(Received 13 April 2016; published 5 July 2016)

Using the convergent close-coupling theory we study the threshold behavior of cross sections for positronium (Ps) of energy  $E$  scattering on antiprotons. In the case of Ps( $1s$ ) elastic scattering, simple power laws are observed for all partial waves studied. The partial-wave summed cross section is nearly constant, and dominates the antihydrogen formation cross section at all considered energies, even though the latter is exothermic and behaves as  $1/E^{1/2}$ . For Ps( $2s$ ), oscillations spanning orders of magnitude on top of the  $1/E$  behavior are found in the elastic and quasielastic cross sections. The antihydrogen formation is influenced by dipole-supported resonances below the threshold of inelastic processes. Resonance energies form a geometric progression relative to the threshold. The exothermic antihydrogen formation cross sections behave as  $1/E$  at low energies, but are oscillation free. We demonstrate that all these rich features are reproduced by the threshold theory developed by Gailitis [J. Phys. B: At. Mol. Phys. **15**, 3423 (1982)].

DOI: [10.1103/PhysRevA.94.012701](https://doi.org/10.1103/PhysRevA.94.012701)**I. INTRODUCTION**

Antihydrogen formation is presently an active experimental program with the aim of performing gravitational and spectroscopic measurements [1]. Using the two-center convergent close-coupling (CCC) method [2] the cross sections for antihydrogen formation via positronium (Ps) scattering on antiprotons have been calculated at low energies for various initial Ps( $nl$ ) states [3,4]. Simple power laws for near-threshold behavior were identified. Here we study the threshold behavior of the underlying partial-wave cross sections utilizing the most general treatment of such collision processes given by Gailitis [5]. In addition to the antihydrogen formation, the elastic and quasielastic ( $l$  changing for same  $n$ ) cross sections are considered. We demonstrate that all of the remarkably rich near-threshold behavior can be reproduced using the Gailitis theory.

Hydrogen and hydrogenlike atoms in excited states possess nonzero dipole moment due to the degeneracy of  $nl$  states,  $l = 0, 1, \dots, n - 1$ . This leads to the threshold behavior of the scattering cross sections which differs from the well-known Wigner threshold law [6]. In particular the electron-impact excitation cross sections for the hydrogen atom are finite at the excitation threshold and all cross sections oscillate below and above the threshold [7,8]. Oscillations below the threshold are interpreted as resonances due to dipole-supported states. A similar situation occurs when an electron is scattered by a stationary dipole [9] that is relevant to electron scattering by polar molecules. These features are observed as long as splitting between the states interacting by the dipole interaction can be neglected. In the case of electron-hydrogen scattering this means that electron energy should be large compared to the Lamb shift.

Gailitis [5] developed a more general theory relevant to interaction of a charged particle with a hydrogenlike system, of which Ps +  $p$  is an example. In the present application of this theory we are interested in collision processes involving Ps atom in the first excited state

$$\text{Ps}(2l) + p \rightarrow \text{Ps}(2l') + p \quad (1)$$

and

$$\text{Ps}(2l) + p \rightarrow \text{H}(nl') + e^+ \quad (2)$$

The process (2) has the same cross section as the charge-conjugated reaction

$$\text{Ps}(2l) + \bar{p} \rightarrow \bar{\text{H}}(nl') + e^- \quad (3)$$

Here, we shall derive the threshold behavior of the above collision processes from the general theory of Gailitis [5], and compare it with the results of the convergent close-coupling calculations. We utilize atomic units (a.u.) throughout unless stated otherwise.

**II. THRESHOLD THEORY**

The  $S$  matrix for collision of a charged particle with a hydrogenlike system is given by [5,10]

$$S = \exp(i\pi l/2) A \exp(-i\pi \lambda/2) S' \exp(-i\pi \lambda/2) \times A^{-1} \exp(i\pi l/2), \quad (4)$$

where  $l$  is the diagonal matrix of electron orbital angular momenta,

$$\lambda = -\frac{1}{2} + \left(\frac{1}{4} + \Lambda\right)^{1/2},$$

and where  $\Lambda$ ,  $A$  are eigenvalues and eigenvectors of the equation

$$[l(l+1) + 2m_1 d]A = \Lambda A. \quad (5)$$

Here  $m_1$  is the reduced mass of the projectile-target system, and  $d$  is the dipole moment matrix which couples degenerate channels in the hydrogenlike atom, in our case Ps. The dipole moment matrix scales as  $d = d_H/m_2$ , where  $m_2$  is the reduced mass of the hydrogenlike system, and  $d_H$  is the dipole-moment matrix for interaction of electron with hydrogen. In the case of Ps,  $m_2 = 1/2$ . If we neglect the electron mass compared to the proton mass, we obtain  $m_1 = 2$  and  $m_1 d = 4d_H$ . The expression for the matrix  $d_H$  was given by Seaton [11].

The matrix  $S'$  in Eq. (4) is given by

$$S' = 1 + 2ik^{\lambda+1/2} [M - (\tan \pi \lambda + i)k^{2\lambda+1}]^{-1} k^{\lambda+1/2}, \quad (6)$$

where  $k$  is the diagonal matrix of the channel wave numbers and  $M$  is a symmetric matrix which is a meromorphic function of energy. Typically, if there are no near-threshold resonances caused by the short-range interaction, this matrix can be expanded in powers of energy  $E$ . It is kept constant in the first approximation of the threshold theory.

The threshold behavior depends critically on the spectrum of the eigenvalue problem (5). If the lowest  $\Lambda$  is greater than  $-1/4$ , all  $\lambda$  are real and the elements of  $S'$  behave as

$$S'_{ij} = \delta_{ij} + 2ik_i^{\lambda_i+1/2} (M^{-1})_{ij} k_j^{\lambda_j+1/2}. \quad (7)$$

In this case the elastic and quasielastic (that is, corresponding to transitions between channels with degenerate energies) cross sections behave as  $k^{4\lambda_1}$ , and the inelastic cross section is proportional to  $k^{2\lambda_1+1}$  for an endothermic process, and to  $k^{2\lambda_1-1}$  for an exothermic process. The lowest eigenvalue  $\lambda_1$  varies between zero and  $-1/2$  and  $k = [2m(E - E_t)]^{1/2}$ , where  $E_t$  is the threshold energy ( $E_t = 0$  for exothermic processes). If the lowest  $\Lambda$  is less than  $-1/4$ ,  $\lambda_1$  is complex,

$$\lambda_1 = -\frac{1}{2} + i\mu. \quad (8)$$

For elastic and quasielastic processes, the most important matrix element of  $S'$  is given by the expression

$$S'_{11} = \frac{1 + e^{i\phi - \pi\mu} k^{2i\mu}}{1 + e^{i\phi + \pi\mu} k^{2i\mu}}, \quad (9)$$

where  $\phi$  is an energy-independent phase depending on the short-range interaction. All other elements of  $S'$  are given by  $\delta_{ij}$ , but they do contribute to the cross section since, according to Eq. (4),

$$S_{2l,2l'} = \exp[i\pi(l+l')/2] \sum_i A_{li} A_{l'i} S'_{ii} \exp[-i\pi\lambda_i]. \quad (10)$$

Each term in this sum gives an essential contribution, even if  $S'_{ii} = 1$ . As a result, elastic and quasielastic cross sections oscillate and diverge as  $1/E$ . The oscillations in the cross sections are described by the factor  $\cos(2\mu \ln k + \phi)$ .

In the case of processes (1) and (2)  $\lambda_1$  is complex for  $L \leq 4$ , where  $L$  is the total angular momentum of the system. The corresponding values of  $\mu$  are 4.772, 4.576, 4.155, 3.428, and 2.093 for  $L = 0, 1, 2, 3$ , and 4, respectively.

Note that the discussed features, oscillations, and  $1/E$  divergence of the cross section are observed only for the

“favorable” parity  $P = (-1)^L$  since only in this case we have  $2s - 2p$  coupling producing the dipole interaction. However, for scattering from Ps states with higher  $n$  the features can appear for the “unfavorable” parity  $P = (-1)^{L+1}$  as well.

The situation with inelastic processes is different. The most important  $S$ -matrix element for an inelastic process above the threshold is given by

$$S_{01} = \frac{ck^{i\mu}}{1 + e^{i\phi + \pi\mu} k^{2i\mu}}, \quad (11)$$

where  $c$  is a complex constant and zero denotes a channel with a different energy, not belonging to the degenerate manifold. The phase  $\phi$  is not real in this case, but could be close to real, if the interchannel coupling is weak. The oscillations in the cross section are suppressed in this case by the factor  $\exp(-\pi\mu)$ . Even in the case  $L = 4$ , we obtain  $\exp(-\pi\mu) = 0.0014$ , an insignificant number. However, if we are interested in the cross section below the threshold, for example in Ps( $1s$ ) -  $p$  elastic scattering just below the  $n = 2$  threshold, the corresponding cross section will exhibit pronounced resonances related to the dipole-supported bound states of the Ps -  $p$  system.

For our studies the most important feature of the cross section for an endothermic process is the finite value at the threshold, since  $|S_{01}|^2 \neq 0$  at the threshold. For example, the cross section for the reaction (2) with  $n = 3$ ,



is finite at the threshold  $E_{\text{th}} = 0.5/(2 \times 2^2) - 1/(2 \times 3^2) = 1/144$  a.u. = 0.189 eV. The cross section for an exothermic process, for example the process (2) for  $n \leq 2$ , diverges as  $1/E$  when  $E \rightarrow 0$ .

### III. CONVERGENT CLOSE-COUPPLING THEORY

To test the above threshold theory we compare with the corresponding Ps( $nl$ ) -  $p$  convergent close-coupling (CCC) calculations. Due to the H and Ps centers in the problem we require the two-center CCC formalism [2]. A review of the CCC method for two-center collision systems has been recently given by Kadyrov and Bray [12]. Briefly, Ps-formation channels are explicitly included by adding a second Laguerre-based expansion around the Ps center of mass. Convergence in the calculations are obtained by increasing the Laguerre basis sizes  $N_l^{\text{H}}$  for  $l \leq l_{\text{max}}^{\text{H}}$  and  $N_l^{\text{Ps}}$  for  $l \leq l_{\text{max}}^{\text{Ps}}$ . The other free parameters of the Laguerre basis are the exponential falloffs  $\lambda_l$ . To reduce the number of free parameters we typically take  $\lambda_l = \lambda$  to be optimal for the ground or the first excited state. Furthermore, we typically take  $N_l = N_0 - l$ . Given that the Laguerre basis is complete, its usage with two nonorthogonal expansions is potentially problematic. In practice, the unitarity of the close-coupling theory ensures that there are no double-counting problems, though the numerical equations to be solved become particularly ill-conditioned with increasing  $N_l$ , requiring very accurate numerical methods. However, a major strength of the approach is that its internal consistency with the one-center expansion approach can be readily checked [13,14]. The latter is much more numerically stable, but is unable to distinguish between explicit Ps formation and breakup cross sections. When both methods agree for their sum we can be

very confident in all of the two-center CCC results, which do contain explicit Ps-formation processes.

The CCC parameters used here are the same as those presented earlier [4], except performed on a sufficiently dense energy mesh to elucidate the underlying structures, and extended to partial waves  $L \leq 80$ . The latter is necessary to yield convergent integrated elastic cross sections. The Laguerre basis parameters are  $N_l^H = N_l^{Ps} = 12 - l$  with  $\lambda_l^H = 1.0$  and  $\lambda_l^{Ps} = 0.5$ . We set  $l_{\max}^H = 3$  and  $l_{\max}^{Ps} = 2$ , which allowed the CCC calculations to yield convergent results for Ps( $n \leq 3$ ) to H( $n \leq 4$ ) states [4].

Though  $N_0 = 12$  is not a particularly large basis size the resulting close-coupling equations are sufficiently ill conditioned that yielding stable results in individual partial waves in the vicinity of resonances required a different numerical approach. The recently developed analytical treatment of the Green's function in the solution of the coupled Lippmann-Schwinger equations [15,16] was necessary to yield the required numerical stability. In fact, the new numerical approach shows promise of being able to solve the larger set of coupled equations arising from  $N_l^H = N_l^{Ps} = 15 - l$ , yielding accurate cross sections for Ps( $n \leq 4$ ) to H( $n \leq 5$ ) transitions [16].

## IV. RESULTS

### A. Approximation of $2s - 2p$ degeneracy

We will first present the results obtained with the assumption that the  $2s$  and  $2p$  states are completely degenerate.

In Fig. 1 we present partial-wave and partial-wave summed cross sections for elastic Ps( $2s$ ) +  $p$  scattering calculated using Eqs. (9) and (10), and compare them with the corresponding results of the *ab initio* CCC calculations. The phase  $\phi$  in Eq. (9) has been adjusted for visual fit of the threshold theory cross sections to those of CCC, yielding excellent agreement for the massively oscillating cross sections on top of the  $1/E$  behavior. In contrast, the H-formation cross section has only the  $1/E$  functional form near threshold, and of a substantially lower magnitude than the elastic cross section.

In Fig. 2 we present partial cross sections for Ps( $2s$ ) +  $p \rightarrow$  Ps( $2p$ ) +  $p$  quasielastic collisions exhibiting even more pronounced oscillations. In the approximation of the  $2s - 2p$  degeneracy the total (summed over all  $L$ ) cross section is divergent. This problem is addressed in the following subsection.

In Fig. 3 we show Ps( $1s$ ) +  $p$  scattering cross sections, where the dipole interaction does not play a role at low energies, contrasting them with the Ps( $2s$ ) case. Elastic scattering is controlled by the polarization interaction  $-\alpha/2r^4$ , and, according to the theory of O'Malley *et al.* [17], the partial cross section is constant for  $L = 0$ , and behaves as  $C_L E$  for  $L \geq 1$ , where

$$C_L = \frac{8\pi\alpha^2}{(2L-1)^2(2L+1)(2L+3)^2}, \quad (12)$$

and where  $\alpha = 36$  a.u. is the polarizability of Ps in the ground state. Remarkably, even at the lowest considered energy, the H-formation cross section, despite the Wigner  $1/E^{1/2}$  divergence, remains well below the elastic cross section, with the latter being nearly constant due to the dominant zeroth partial wave.

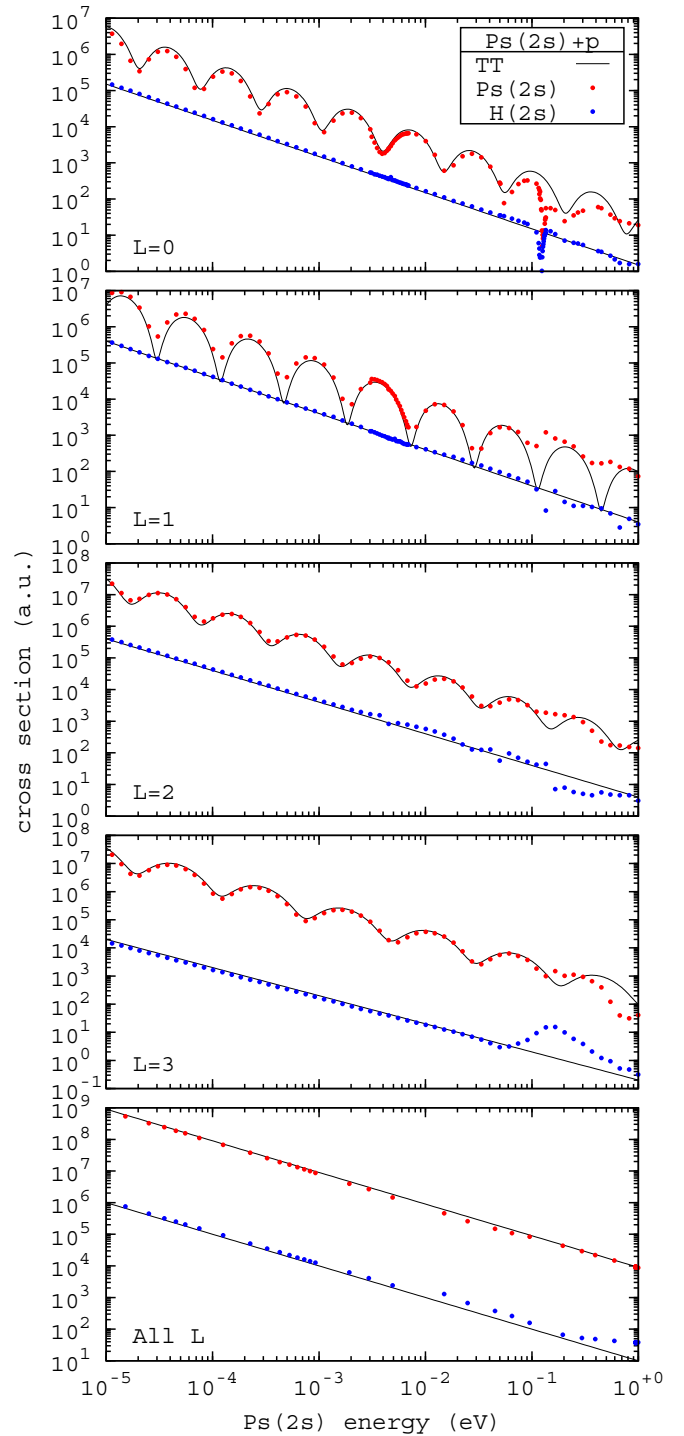


FIG. 1. Partial-wave and partial-wave summed cross sections for Ps( $2s$ ) +  $p$  elastic scattering and H( $2s$ ) production calculated using the convergent close-coupling method (circles) and the threshold theory (TT, lines).

### B. Influence of the $2s - 2p$ splitting

If the Ps  $2s$  and  $2p$  states are completely degenerate (as assumed in the present CCC calculations), then on the log energy scale oscillations would extend to  $-\infty$ . However, because of the relativistic splitting between the  $2s$  and  $2p$  states, the oscillations are limited from below. For example,

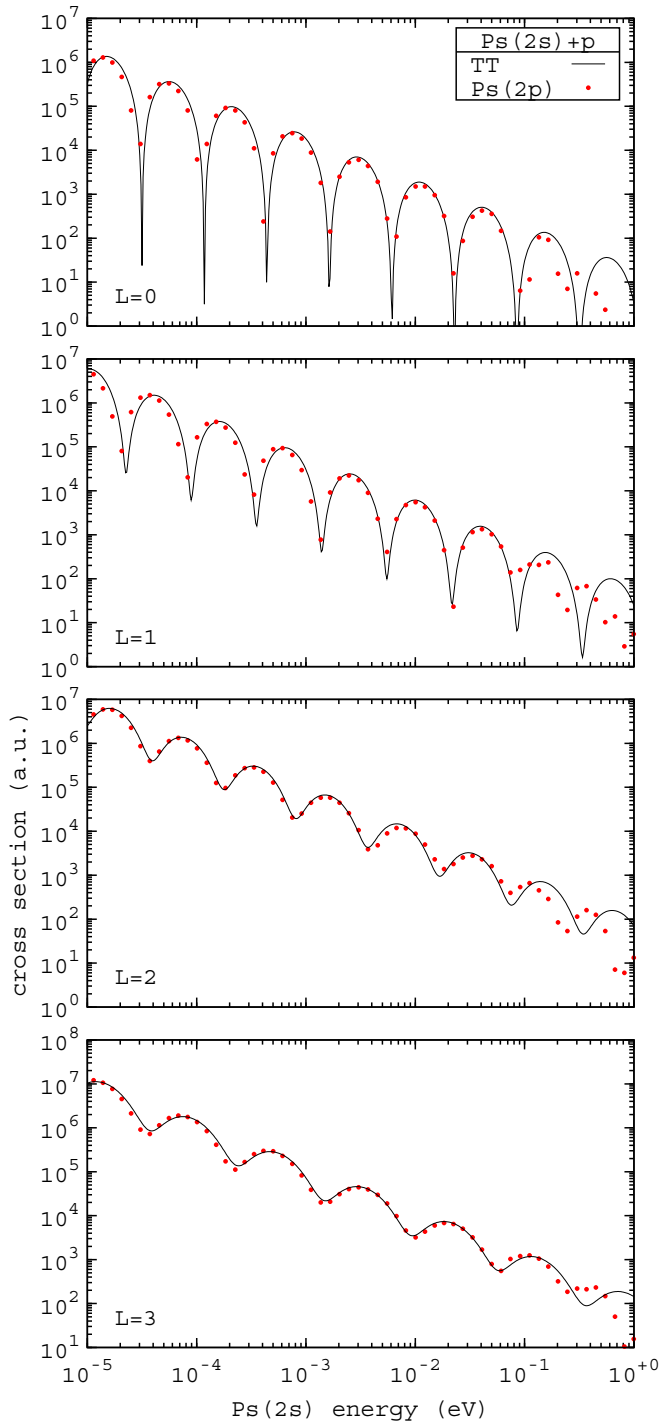


FIG. 2. Partial-wave cross sections for  $\text{Ps}(2s) + p \rightarrow \text{Ps}(2p) + p$  quasielastic scattering calculated using the convergent close-coupling method (circles) and the threshold theory (TT, lines).

the splitting between  $2^3P_1$  and  $2^3S_1$  states in ortho-Ps is about  $13 \text{ GHz} = 5.4 \times 10^{-5} \text{ eV}$  [18,19], and this means that the oscillations stop at  $\log_{10} E < -4$ . Moreover, the Wigner threshold law should be restored in this energy range meaning that the cross section behaves as  $k^{4l}$  for pure elastic scattering, where  $l$  is the lowest electron angular momentum allowed for a given symmetry. The quasielastic cross section in this region

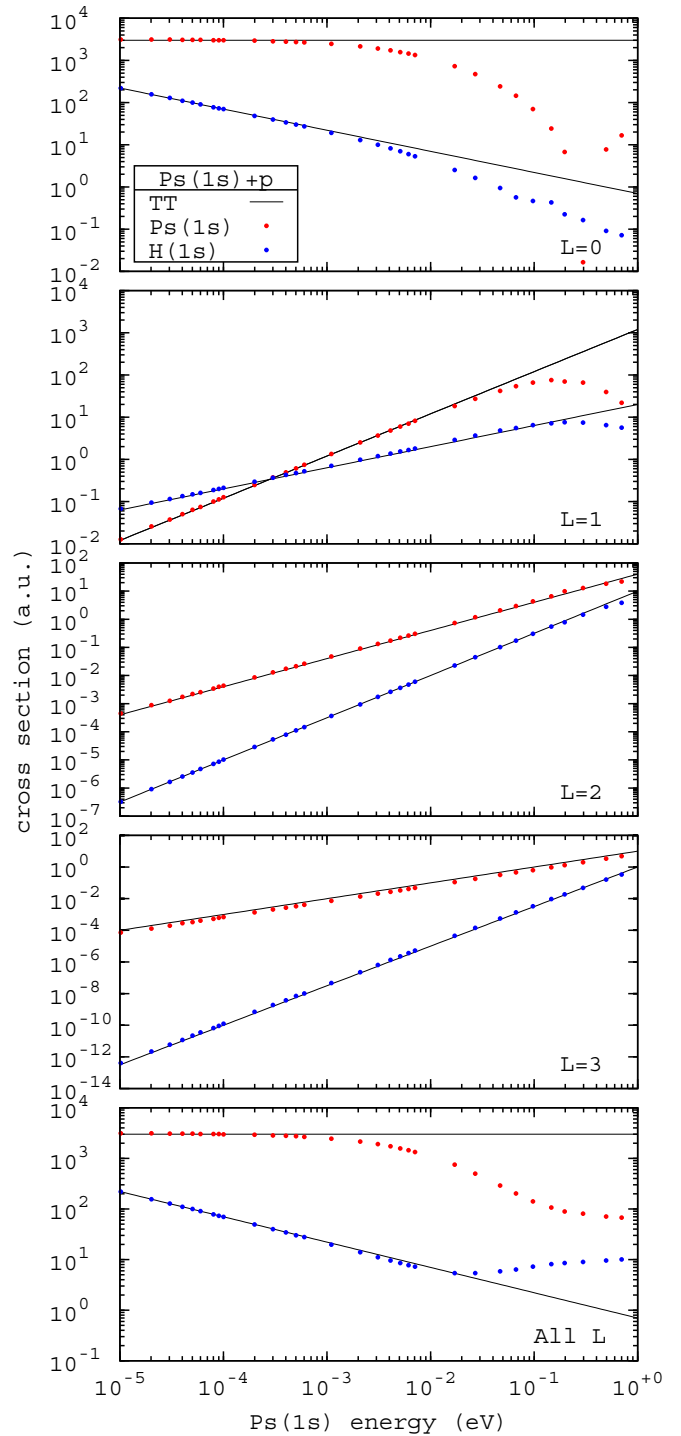


FIG. 3. Same as for Fig. 1, except for  $\text{Ps}(1s) + p$  scattering.

behaves as  $k_i^{2l_i-1} k_f^{2l_f+1}$ , where  $k_i, k_f$  are the initial and final wave numbers, and  $l_i, l_f$  are corresponding angular momenta.

From the high-energy side the oscillations are limited by the condition of the validity of the threshold theory. This can be estimated as  $k < 1/R$ , where  $R$  is the radius of the short-range interaction (about the size of the Ps atom).

The relativistic splitting also affects the convergence of the partial-wave summed cross sections. For their calculation higher angular momenta should be included. The  $T$  matrix at

large  $L$  depends only on the dipole interaction and was given by Gailitis [20] for electron scattering by the excited hydrogen atom. For Ps- $p$  scattering it should be multiplied by the factor  $m_1/m_2 = 4$ . Accordingly,

$$\begin{aligned} T_{2sL \rightarrow 2sL} &= 24 \frac{3}{L(L+1)}, \\ T_{2sL \rightarrow 2pL-1} &= 24 \frac{i}{[L(2L+1)]^{1/2}}, \\ T_{2sL \rightarrow 2pL+1} &= 24 \frac{-i}{[(L+1)(2L+1)]^{1/2}}, \end{aligned} \quad (13)$$

and

$$\begin{aligned} T_{2pL \mp 1 \rightarrow 2pL \mp 1} \\ = 24 \left[ \begin{array}{cc} \frac{3}{2L+1} \left( \frac{-i\pi}{2L-1} + \frac{1}{L} \right) & \frac{-3}{(2L+1)[L(L+1)]^{1/2}} \\ \frac{-3}{(2L+1)[L(L+1)]^{1/2}} & \frac{3}{2L+1} \left( \frac{i\pi}{2L+3} - \frac{1}{L+1} \right) \end{array} \right], \end{aligned} \quad (14)$$

where, for example, the top right element corresponds to the  $L-1 \rightarrow L+1$  transition.

It follows from these expressions that the partial-wave expansion for the  $2s \rightarrow 2s$  and  $2p \rightarrow 2p$  cross sections [ $\sigma_L \propto (2L+1)|T_L|^2$ ] converges as  $1/L^3$ , whereas the cross section for the quasielastic transition  $2s \rightarrow 2p$  diverges as a  $1/L$  harmonic series. This is all assuming that the relativistic splitting between  $2s$  and  $2p$  is neglected, and is a well-known result for scattering in the presence of dipole coupling between degenerate states. The same situation also occurs in scattering by a stationary dipole [21]. To remedy this situation, scattering by a rotating dipole in the Born approximation for higher partial waves is included [22]. As a result, the harmonic series is replaced by the factor  $\ln(4E/\Delta E)$ , where  $\Delta E$  is the splitting between the dipole-coupled states. This factor is related to an effective cutoff in  $L$  beyond which scattering becomes insignificant. Indeed, the collision time can be estimated as  $t \sim \rho/v = L/2E$ , where  $\rho$  is the impact parameter and  $v$  is the projectile velocity. The collision is efficient if  $t < 1/\Delta E$ , and this leads to the effective cutoff in  $L$ ,

$$L_{\text{cut}} = \frac{2E}{\Delta E}. \quad (15)$$

This estimate is valid up to a numerical factor of the order of 1. However, its exact value is not really important because of the fast convergence of the elastic cross section and the logarithmic divergence of the quasielastic cross section. We can now use this estimate to calculate Ps( $2l$ ) +  $p$  cross section by summing partial waves up to  $L_{\text{cut}}$ . Naturally, the whole procedure is valid only for  $E \gg \Delta E$ . For energies comparable to the relativistic splitting numerical solution of coupled equations with the account of the splitting is necessary.

Calculations according to this scheme are presented in Fig. 4, where we plot the product  $\sigma E$  for all three partial-wave summed cross sections. Here, the available  $L \leq 80$  CCC-calculated partial cross sections were summed up to  $L_{\text{cut}}$ , which ranges from 3 at  $10^{-4}$  eV to 40000 at 1 eV, with the  $L > 80$  partial cross sections coming from the use of Eqs. (13) and (14). The oscillations in the partial-wave summed cross sections, seen in Figs. 1 and 2 for low partial waves, almost completely disappear because of a significant background due to  $L > 4$ . However, a remnant of oscillatory

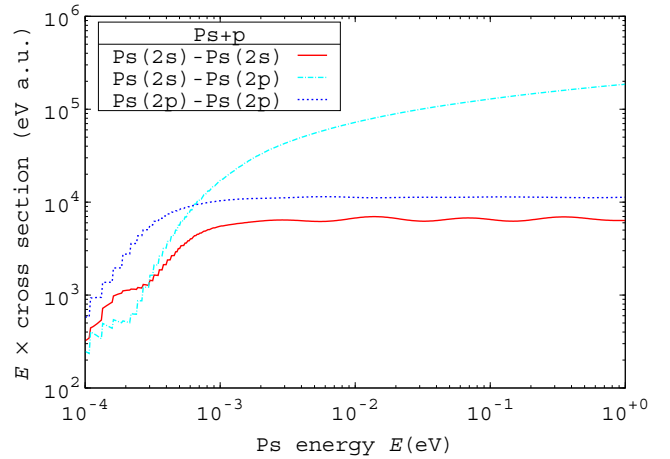


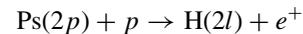
FIG. 4. Partial wave summed to  $L_{\text{cut}}$  cross sections multiplied by collision energy  $E$  for Ps( $2l$ ) +  $p \rightarrow$  Ps( $2l'$ ) +  $p$  scattering; see text.

behavior is still seen in the elastic cross sections. Additionally, these oscillations should be observable in the differential cross sections as a function of energy at large scattering angles. At energies below 0.001 eV the wiggling structures are an artifact of  $L_{\text{cut}}$  being an integer. The purpose of showing the low energy results here is solely to demonstrate that the threshold behavior changes if  $\Delta E \neq 0$ . The uncertainties become negligible in the energy range above  $10^{-3}$  eV. In the region between 0.003 and 1 eV elastic cross sections behave as  $A/E$ , where  $A$  is a slowly varying function of energy whose typical values, say, at  $E = 0.01$  eV, are  $6707a_0^2$  eV for scattering in the  $2s$  state, and  $11219a_0^2$  eV for scattering in the  $2p$  state. For the quasielastic  $2s \rightarrow 2p$  transition the cross section behaves as  $B \ln E/E$ , where  $B$  is another slowly varying function of  $E$ , with  $B \ln E = 55173a_0^2$  eV at  $E = 0.01$  eV. The conclusion important for experiments is that all cross sections are very large, and the  $2s \rightarrow 2p$  cross section dominates above 0.001 eV.

### C. Reaction cross sections

The cross section for an endothermic process involving excited Ps should be finite at the threshold, and diverge as  $1/E$  in the exothermic case, if the dipole coupling is present. In addition, resonances due to dipole-supported states should be observed below higher-energy thresholds.

As an example, consider the exothermic reaction



in the vicinity of the H( $3l$ ) formation threshold energy 0.189 eV. In Fig. 5 we show the  $L = 3$  partial cross sections. Formation of H( $2p$ ) can occur for two parities:  $P = +1$  (“unfavorable” parity) and  $P = -1$  (“favorable” parity). The low-energy behavior is influenced by the dipole coupling in the H( $2s$ ) and H( $2p$ )  $P = -1$  cases, and therefore the cross section diverges as  $1/E$ . In contrast, for the H( $2p$ )  $P = +1$  case the dipole coupling is absent, and the threshold behavior is instead given by the Wigner law  $\sigma \propto E^{2.5}$ . As follows from the general theory, the low-energy oscillations are suppressed. Instead, the  $P = -1$  cross section exhibits two dipole-supported resonances just below the H( $3l$ ) +  $e^+$  threshold. According

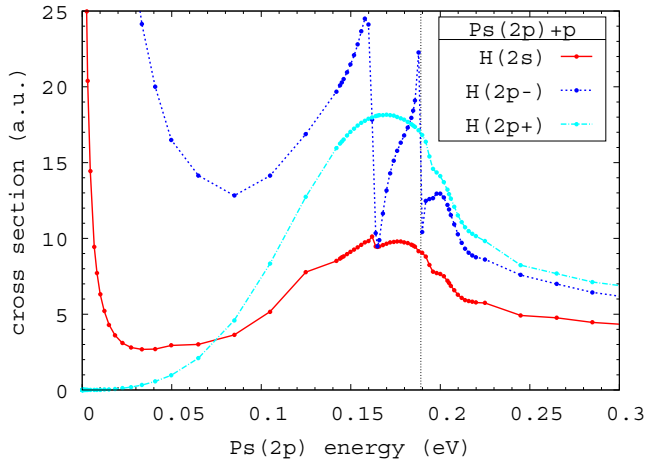


FIG. 5. Cross section for the reaction  $\text{Ps}(2p) + p \rightarrow \text{H}(2l) + e^+$  for  $L = 3$  calculated using the convergent close-coupling method. The sign following the  $2p$  label indicates parity  $P$ . The dotted vertical line indicates the  $\text{H}(n = 3)$  threshold of 0.189 eV.

to the general theory [5], the dipole coupling is sufficient to produce resonances only in the  $P = -1$  case. In the approximation of the  $3s - 3p - 3d$  degeneracy, the position of these resonances relative to the threshold form an infinite geometric progression with the common ratio

$$1/R = \exp\left[-\frac{2\pi}{\mu}\right], \quad (16)$$

where  $\mu$  is determined from the solution of the eigenvalue problem, Eq. (5), and Eq. (8). For the  $\text{H}(3l) + e^+$  threshold for  $L = 3$  we have  $R = 9.3227$  [5]. From the calculations presented in Fig. 5 we estimate the distances of the first and second resonances to the  $n = 3$  threshold to be 0.029 eV and 0.003 eV, respectively, yielding  $R \approx 9.67$  in good agreement

with the above prediction. In reality the number of resonances is limited because of the relativistic splitting. Similar, but less pronounced, resonances are observed in the  $\text{Ps}(2p) + p \rightarrow \text{H}(2s) + e^+$  process. Their relative weakness is due to the weaker coupling between the  $n = 3$  dipole-supported state and the  $\text{H}(2s)$  state.

## V. CONCLUSIONS

In conclusion, we have demonstrated several remarkable features in  $\text{Ps} - p$  and equivalently  $\text{Ps} - \bar{p}$  collisions near-threshold cross sections. Using the CCC method, very large oscillations were found for low partial waves in elastic and quasielastic scattering for  $\text{Ps}(2s)$  initial states. According to the threshold theory of Gailitis, these are due to the dipole coupling between degenerate states in excited Ps and excited (anti)hydrogen. Below-threshold dipole-supported resonances in inelastic processes, and  $1/E$  divergences of the cross sections for elastic and some inelastic processes were also found, as predicted by Gailitis. The CCC-calculated elastic cross sections were found to be particularly large, around three orders of magnitude bigger than the corresponding (anti)hydrogen formation cross sections. The implication of this for the antihydrogen formation experimental program will be discussed elsewhere [23].

## ACKNOWLEDGMENTS

We thank Mike Charlton for many useful discussions. This work has been supported by the US National Science Foundation under Grant No. PHY-1401788, the Australian Research Council, and the Pawsey Supercomputing Centre with funding from the Australian Government and the Government of Western Australia. A.S.K. acknowledges partial support from the US National Science Foundation under Grant No. PHY-1415656.

- 
- [1] M. Charlton and D. P. Van Der Werf, *Sci. Prog.* **98**, 34 (2015).
  - [2] A. S. Kadyrov and I. Bray, *Phys. Rev. A* **66**, 012710 (2002).
  - [3] A. S. Kadyrov, C. M. Rawlins, A. T. Stelbovics, I. Bray, and M. Charlton, *Phys. Rev. Lett.* **114**, 183201 (2015).
  - [4] C. M. Rawlins, A. S. Kadyrov, A. T. Stelbovics, I. Bray, and M. Charlton, *Phys. Rev. A* **93**, 012709 (2016).
  - [5] M. Gailitis, *J. Phys. B: At. Mol. Phys.* **15**, 3423 (1982).
  - [6] E. P. Wigner, *Phys. Rev.* **73**, 1002 (1948).
  - [7] M. Gailitis and R. Damburg, *Zh. Eksp. Teor. Fiz.* **44**, 1644 (1963) [*Sov. Phys. JETP* **17**, 1107 (1963)].
  - [8] M. Gailitis and R. Damburg, *Proc. Phys. Soc.* **82**, 192 (1963).
  - [9] I. I. Fabrikant, *Zh. Eksp. Teor. Fiz.* **73**, 1317 (1977) [*Sov. Phys. JETP* **46**, 693 (1977)].
  - [10] I. I. Fabrikant, *J. Phys. B: At. Mol. Phys.* **12**, 3599 (1979).
  - [11] M. J. Seaton, *Proc. Phys. Soc.* **77**, 174 (1961).
  - [12] A. S. Kadyrov and I. Bray (unpublished).
  - [13] J. J. Bailey, A. S. Kadyrov, and I. Bray, *Phys. Rev. A* **91**, 012712 (2015).
  - [14] I. Bray, J. J. Bailey, D. V. Fursa, A. S. Kadyrov, and R. Utamuratov, *Eur. Phys. J. D* **70**, 6 (2016).
  - [15] A. W. Bray, I. B. Abdurakhmanov, A. S. Kadyrov, D. V. Fursa, and I. Bray, *Comput. Phys. Commun.* **196**, 276 (2015).
  - [16] A. W. Bray, I. B. Abdurakhmanov, A. S. Kadyrov, D. V. Fursa, and I. Bray, *Comput. Phys. Commun.* **203**, 147 (2016).
  - [17] T. F. O'Malley, L. Spruch, and L. Rosenberg, *J. Math. Phys.* **2**, 491 (1961).
  - [18] S. Hatamian, R. S. Conti, and A. Rich, *Phys. Rev. Lett.* **58**, 1833 (1987).
  - [19] E. W. Hagena, R. Ley, D. Weil, G. Werth, W. Arnold, and H. Schneider, *Phys. Rev. Lett.* **72**, 2887 (1994).
  - [20] M. Gailitis, *J. Phys. B: At. Mol. Phys.* **11**, L279 (1978).
  - [21] W. R. Garrett, *Phys. Rev. A* **4**, 2229 (1971).
  - [22] I. I. Fabrikant, *Zh. Eksp. Teor. Fiz.* **71**, 148 (1976) [*Sov. Phys. JETP* **44**, 77 (1976)].
  - [23] M. Charlton, A. S. Kadyrov, and I. Bray (unpublished).